

# A Wide-Band High Isolation Dual-Circularly Polarized Microstrip Antenna Array

Shiqiang Fu<sup>\*</sup>, Pengfei Liang, Chanjuan Li, and Zhongbao Wang

**Abstract**—A wide-band dual-circularly polarized transceiver antenna with high port isolation is proposed in this paper. The antenna element uses M-shaped and U-shaped microstrip lines to excite the quasi-cross-shaped aperture to achieve wide-band and lower cross-polarization level. Dual-circular polarization is accomplished via the sequential rotation technique. To obtain high port isolation of the antenna, phase cancellation technique and decoupling structure are utilized. The measurements show that the impedance bandwidth with reflection coefficient less than  $-10$  dB is larger than 34.5% (4.6–6.5 GHz) for left-hand circular polarization (LHCP) port and 29.8% (4.86–6.5 GHz) for right-hand circular polarization (RHCP) port, while the 3 dB axial ratio bandwidth for LHCP and RHCP is greater than 29.1% (4.8–6.4 GHz) and 32.7% (4.7–6.5 GHz), respectively. The port isolation of the antenna is higher than 30 dB in 4.5–6.5 GHz band. The peak gain is about 12 dBic.

## 1. INTRODUCTION

Microwave radar has been popular in short-range applications in recent years because of high precision, noninvasiveness, and noncontact [1]. The Frequency Modulated Continuous Wave (FMCW) radar, a type of microwave radar, is utilized more and more frequently in daily life like automotive applications [2], present gesture detection [3], vital sign detection [4], etc. The FMCW radar market is expanding. However, insufficient transceiver isolation will cause signal-to-noise ratio (SNR) to deteriorate and signal processing to become more difficult. These radar transceivers are susceptible to interference due to the mutual coupling of the transmitting (TX) and receiving (RX) antennas. In practice, TX and RX antennas are typically separated from each other to meet the isolation requirement for applications. However, in order to make the radar transceivers more compact, TX and RX antennas can share a single antenna aperture. Circularly polarized (CP) antennas have the advantages of resisting multipath interference and reducing polarization mismatch loss. Moreover, spatial coupling can be avoided when dual-CP antennas are used as transceiver antennas. Therefore, it is necessary to design a wide-band dual-CP single-antenna with high port isolation for radar sensing.

Currently, numerous studies have been conducted on the CP antenna with high port isolation. References [5, 6] both proposed a wide-band single-CP antenna with the port isolation greater than 40 dB in the operating frequency band, but only RHCP was realized. Most researches about dual-CP antennas with high port isolation can be divided into two categories: one is dual-CP in dual-bands, and the other is dual-CP in the same band. The antennas proposed in [7–9] adopted radiation patches that work in different frequencies and obtained dual-CP by phase control. To the best knowledge of the authors, there has been fewer designs on dual-CP antennas in the same band than on dual-band dual-CP antennas. A dual-CP antenna with a low profile and wide axial ratio beam based on Substrate Integrated Waveguide (SIW) was designed in [10]. However, the relative bandwidth is only 7.69%. Although a wide-band dual-CP antenna employing meta-surface technology was presented in [11], inadequate port isolation

---

*Received 26 November 2022, Accepted 14 February 2023, Scheduled 28 February 2023*

<sup>\*</sup> Corresponding author: Shiqiang Fu (fushq@dlmu.edu.cn).

The authors are with the School of Information Science and Technology, Dalian Maritime University, Dalian, Liaoning, China.

remains an issue. Reference [12] proposed a wide-band dual-CP antenna that used neutralization lines to improve isolation. However, the port isolation is just barely above 17 dB. In [13], a dual-CP microstrip antenna with high isolation based on hybrid ring feeding was proposed. Nevertheless, the band was narrow. A dual-CP transceiver antenna was proposed in [14]. The wide band was realized, and the high port isolation was obtained, but the gain in the operating frequency band was only about 6 dB.

In this letter, a wide-band dual-CP antenna array with high port isolation in the same band is proposed. The element antenna adopts aperture-coupled feeding method to enhance the impedance matching bandwidth, and it can radiate linearly polarized wave with lower cross-polarization level by using quasi-cross-shaped slot pair feed. Circular polarization is achieved by sequential rotation array of linearly polarized element antenna. By selecting different excitation ports, LHCP and RHCP can be realized. The array adopts phase cancellation technology and decoupling structures to obtain high port isolation in the 4.5–6.5 GHz band. The complete analysis procedure and the final measured results are provided to demonstrate the viability of the proposed antenna. The configuration and design procedure of the proposed antenna are introduced in Section 2. In Section 3, the fabricated antenna prototype is shown, and experimental results are given. Finally, the conclusion is made in Section 4.

## 2. ANTENNA DESIGN

The proposed antenna array is composed of three substrates as shown in Fig. 1(a). The top substrate is FR4 ( $\epsilon_r = 4.4$ ) with a thickness of 0.6 mm. Arch-shaped decoupling structures are etched on the top side of FR4 substrate, and H-shaped decoupling structures and four radiation patches are placed

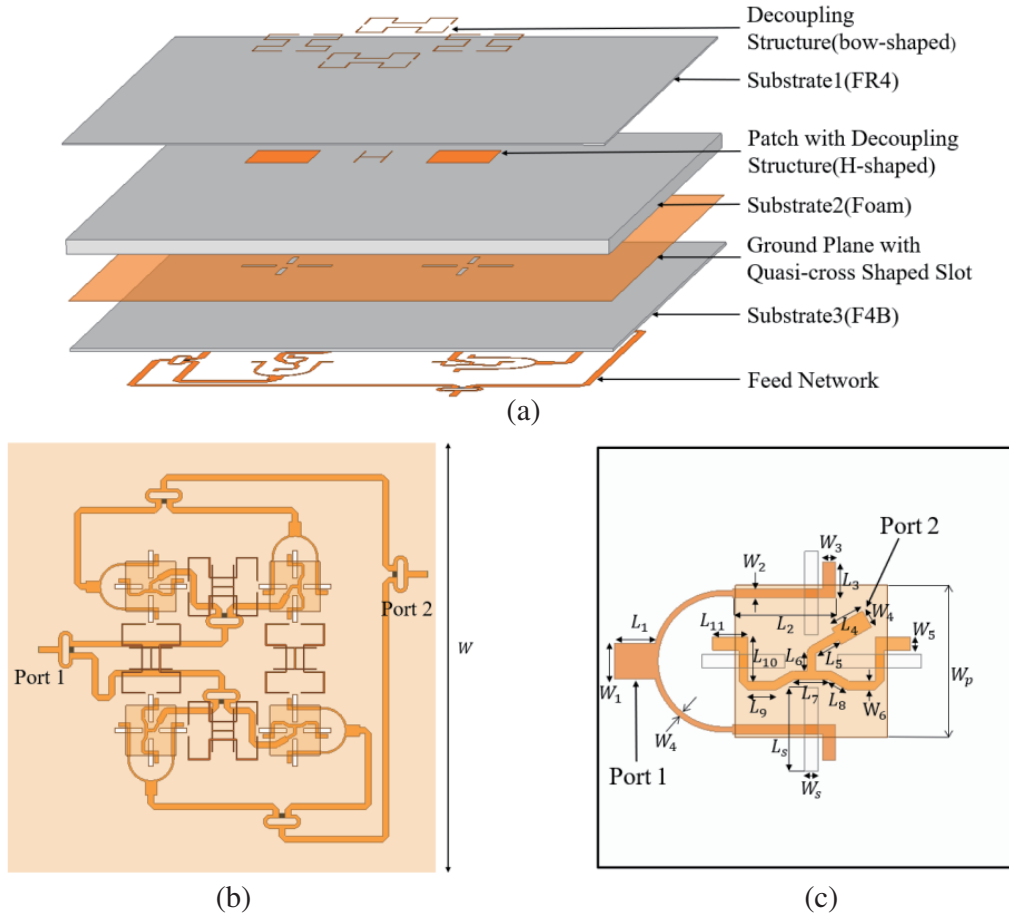


**Figure 1.** Configuration of the proposed antenna. (a) Exploded view. (b) Top view. (c) Enlarged view.

on the bottom side. The middle substrate is foam with a thickness of 4 mm which is used to increase bandwidth and provide support. The bottom substrate is F4B ( $\epsilon_r = 2.65$ ) with a thickness of 0.8 mm. The ground plane with a quasi-cross-shaped slot is placed on the top side of F4B substrate. The feed network in Fig. 1(b) is designed on the bottom side of the F4B substrate and is employed to provide dual-circular polarization and high port isolation. The array has a total height of 5.4 mm ( $0.09\lambda_0$ ,  $\lambda_0$  is the free-space wavelength at 5.5 GHz). The antenna element is shown in Fig. 1(c). The patch is excited through the quasi-cross-shaped slot. The quasi-cross-shaped slot consists of four slots, which are arranged symmetrically. The feedlines are designed to be U-shaped and M-shaped to avoid intersections [15]. This method of feeding has the advantage of reducing the discontinuity of the current on the patch surface, thus improving the polarization purity [16].

High Frequency Structure Simulator (HFSS) software is used to optimize the antenna parameters for better impedance matching and greater port isolation. The final parameters are described as follows:  $W_1 = 4$  mm,  $L_1 = 5$  mm,  $W_2 = 1$  mm,  $W_3 = 1.5$  mm,  $W_4 = 2.1$  mm,  $W_5 = 1.5$  mm,  $L_2 = 10.25$  mm,  $L_3 = 4$  mm,  $L_4 = 4$  mm,  $L_5 = 3$  mm,  $L_6 = 2$  mm,  $L_7 = 4.05$  mm,  $L_8 = 2$  mm,  $L_9 = 3$  mm,  $L_{10} = 4.5$  mm,  $L_{11} = 4$  mm,  $L_s = 9.5$  mm,  $W_s = 1.5$  mm,  $W_p = 17.3$  mm,  $W = 120$  mm. Simulation results of  $S$ -

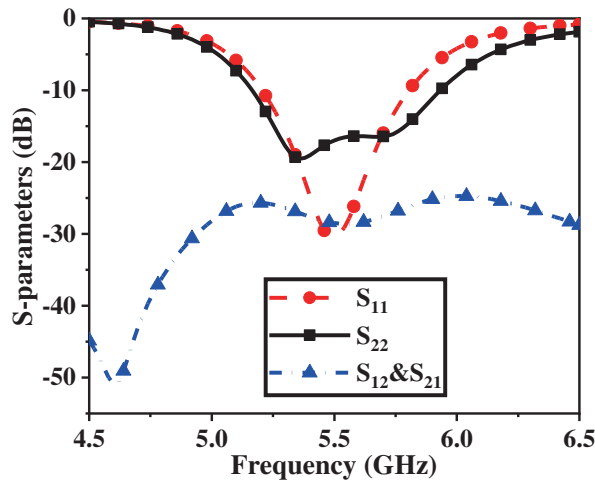


Figure 2.  $S$ -parameters of the antenna element.

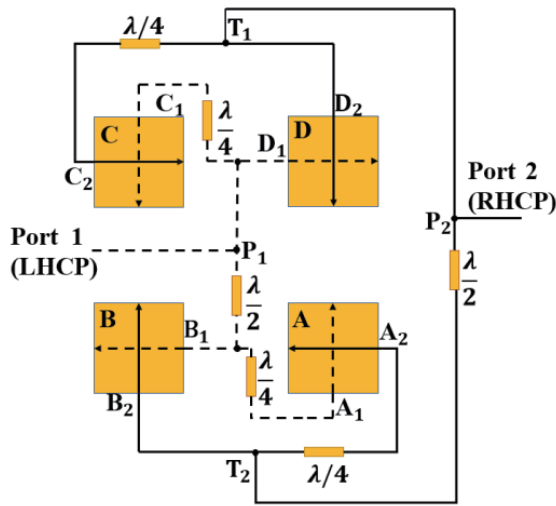


Figure 3. Schematic of the dual-CP antenna array.

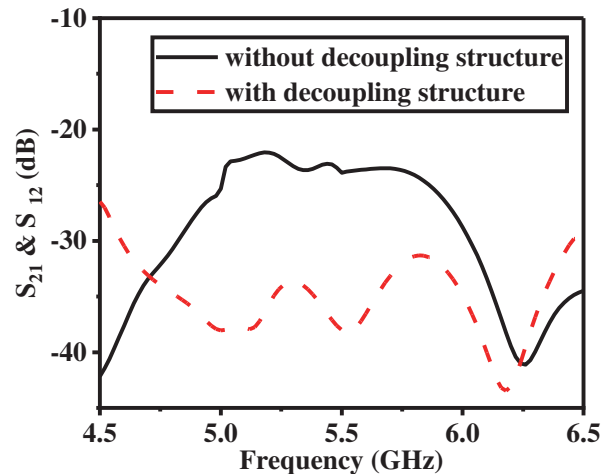
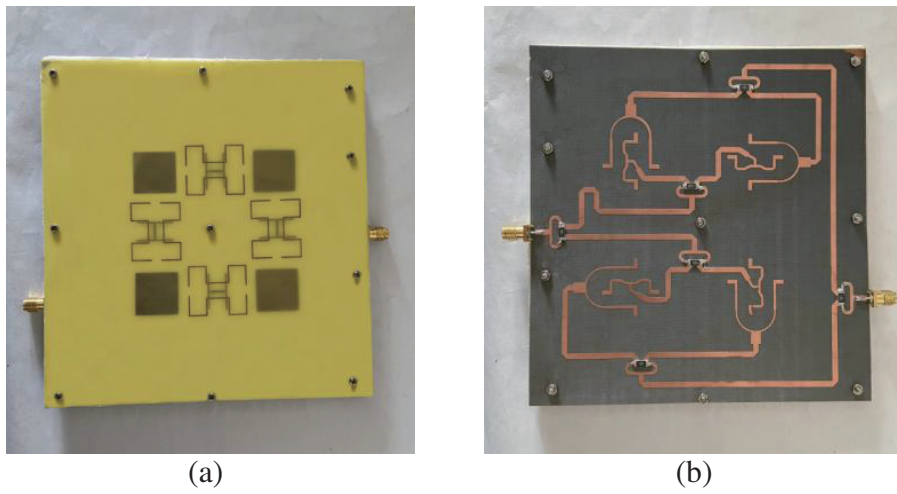


Figure 4. Curves of two-port isolation.

parameters of an element antenna are shown in Fig. 2. The simulated  $|S_{11}| \leq -10$  dB bandwidths of the antenna are 5.21–5.81 GHz for port 1 and 5.16–5.93 GHz for port 2. From 4.5 to 6.5 GHz, the port isolation is greater than 25 dB.

The antenna array is constructed by sequential rotation as depicted in Fig. 3. When port 1 or 2 is excited, the four patches A, B, C, and D are fed by  $-270^\circ$ ,  $-180^\circ$ ,  $-90^\circ$ , and  $0^\circ$  to realize circular polarization. The antenna implements LHCP on port 1 and RHCP on port 2. More importantly, when port 1 is activated, the coupled signals from patch C and patch D to port 2 are out of phase and cancel each other out at  $T_1$  point. The same goes for patch A and patch B at  $T_2$  point. As a result, the port isolation of the antenna array can be infinite in theory. However, due to the space mutual coupling between the four patches, the isolation will be limited. In order to reduce the mutual coupling effect between the patches, H-shaped and arch-shaped microstrip lines are introduced between them [17]. As demonstrated in Fig. 4, the decoupling structure greatly improves the port isolation of the antenna, which increases by nearly 17 dB at the center frequency of 5.5 GHz.



**Figure 5.** Photograph of the fabricated antenna prototype. (a) Top view. (b) Bottom view.

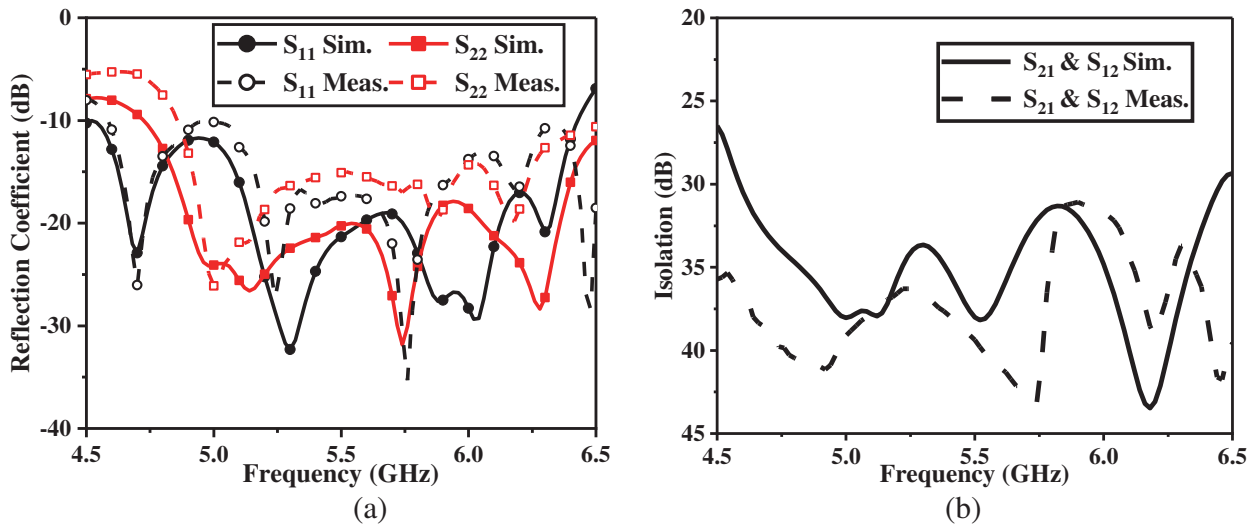


**Figure 6.** Simulated and measured  $S$ -parameters of the proposed antenna. (a) Reflection Coefficient. (b) Isolation.

### 3. EXPERIMENTAL RESULTS

The fabricated antenna prototype can be seen in Fig. 5. Tests on the reflection coefficient and port isolation of the antenna were conducted using an Agilent N5230A vector network analyzer. The simulated and measured results of the proposed antenna are shown in Fig. 6. The antenna's impedance bandwidth with  $|S_{11}| \leq -10$  dB is 4.6–6.5 GHz and  $|S_{22}| \leq -10$  dB is 4.86–6.5 GHz. The relative bandwidth reaches 34.5% and 29.8%, respectively. The port isolation of the antenna in the 4.5–6.5 GHz band is greater than 30 dB. The measured port isolation at 5.5 GHz is 39.4 dB. The differences between the simulated and measured results are mainly attributed to fabrication tolerance and measurement uncertainty.

The gain, axial ratio, and radiation patterns of the antenna were measured in a microwave anechoic chamber. The measured variation curves of gain and axial ratio with frequency are shown in Fig. 7. In

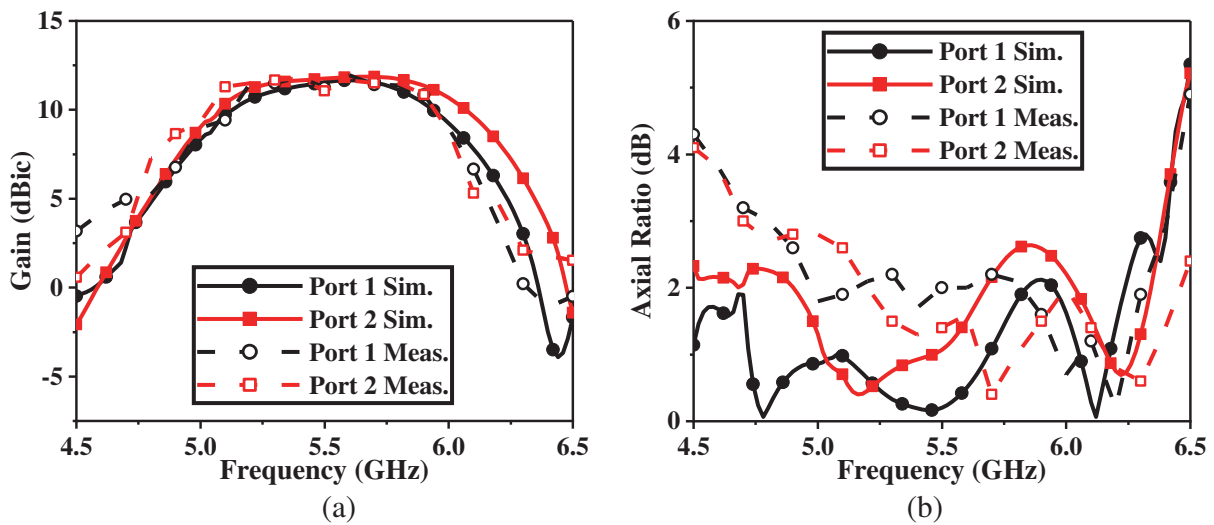


Figure 7. Simulated and measured results of the proposed antenna. (a) Gain. (b) Axial Ratio.

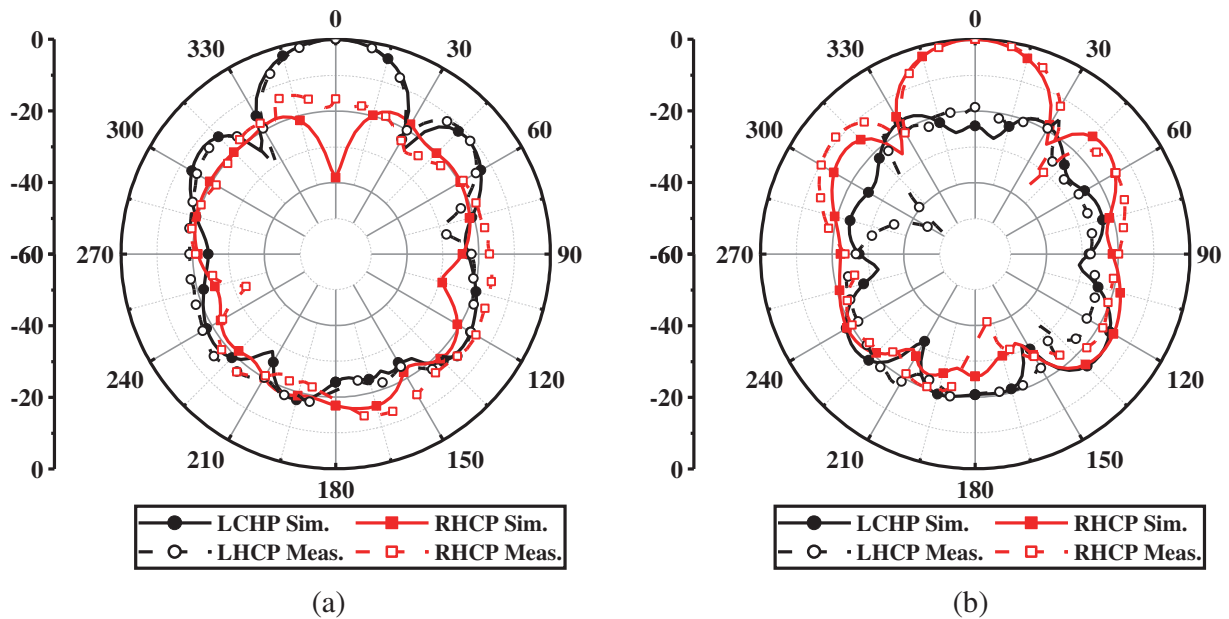


Figure 8. Simulated and measured radiation patterns at 5.5 GHz. (a) Port 1 is excited. (b) Port 2 is excited.

the 5–6 GHz band, the gain is higher than 9 dBic. Peak gains for LHCP and RHCP are 11.9 dBic and 11.8 dBic, respectively, and the respective bandwidths with axial ratio less than 3 dB are 4.8–6.4 GHz and 4.7–6.5 GHz. The antenna radiation patterns of the LHCP and RHCP at 5.5 GHz are shown in Fig. 8. It can be observed that the measured main lobes at center frequency agree well with the simulations. The antenna has good circular polarization radiation performance in the main direction. Some minor discrepancies may be caused by the influence of the test environment and the measurement accuracy of microwave anechoic chamber.

Table 1 presents a contrast between the proposed antenna and reference antennas. The proposed antenna may achieve wide-band dual-CP in comparison to single-CP antennas, which can achieve high port isolation in [5, 6]. In addition, the proposed antenna realizes higher port isolation than other proposed antennas in [10–13, 18]. Compared to the dual-CP antenna with good port isolation in [14], the antenna in this work has a higher gain and a wider bandwidth.

**Table 1.** Comparison of the proposed antenna and reference antennas.

Ref.	Impedance Bandwidth (GHz)	Circular Polarization	Port Isolation (dB)	Peak Gain (dBic)	Size ( $\lambda_0^3$ )
[5]	2.4–2.5	RHCP	> 40.6	7.2	$1.92 \times 1.92 \times 0.016$
[6]	2.4–2.5	RHCP	> 41	10.5	$1 \times 1 \times 0.03$
[10]	4.98–5.42 (8.4%) 4.96–5.43 (9.1%)	LHCP, RHCP	> 16	5.2	$2.2 \times 2 \times 0.1$
[11]	4.33–6.39 (38.4%) 4.17–6.7 (46.6%)	LHCP, RHCP	> 12	7.7	$0.88 \times 0.88 \times 0.06$
[12]	4.65–5.9 (25%)	LHCP, RHCP	> 17	11.3	$0.54 \times 0.54 \times 0.09$
[13]	2.4–2.5	LHCP, RHCP	> 10	3.0	$0.4 \times 0.4 \times 0.025$
[14]	5–6 (18.2%)	LHCP, RHCP	> 35	6.9	$1.33 \times 1.33 \times 0.03$
[18]	4.66–6.31 (30.9%)	LHCP, RHCP	> 14	16	$2.34 \times 2.34 \times 0.07$
This work	4.6–6.5 (34.5%) 4.86–6.5 (29.8%)	LHCP, RHCP	> 30	11.8	$2.3 \times 2.3 \times 0.09$

## 4. CONCLUSION

A dual-CP wideband microstrip antenna array with good port isolation has been presented in this work. By employing U-shaped and M-shaped feedlines to excite a quasi-cross-shaped coupling aperture, an ideal linearly polarized wide-band antenna element with high polarization purity is constructed. Based on the antenna element, the circular polarization array is composed by the sequential rotation technique. Furthermore, the isolation of the antenna is improved by using the decoupling structure in space and the phase cancellation technique in the feed network. The measured results show that the proposed dual-CP antenna array can covers the 5–6 GHz band with gain greater than 9 dBic and isolation higher than 30 dB. For LHCP, the impedance bandwidth with  $|S_{11}| \leq 10$  dB is about 34.5% (4.6–6.5 GHz), and the 3 dB axial ratio bandwidth is about 29.1% (4.8–6.4 GHz). For RHCP, the impedance bandwidth with  $|S_{11}| \leq 10$  dB is about 29.8% (4.86–6.5 GHz), and the 3 dB axial ratio bandwidth is about 32.7% (4.7–6.5 GHz). The measurements and simulations agree fairly well. The antenna has been successfully applied to the FMCW radar system.

## ACKNOWLEDGMENT

National Natural Science Foundation of China, Grant/Award Number: 61871417.

## REFERENCES

1. Li, C., Peng, Z., Huang, T., Fan, T., Wang, F., Horng, T., J. Muñoz-Ferreras, J., Gómez-García, R., Ran, L., and Lin, J., "A review on recent progress of portable short-range noncontact microwave radar systems," *IEEE Transactions on Microwave Theory and Techniques*, Vol. 65, No. 5, 1692–1706, 2017.
2. Venon, A., Y. Dupuis, P. Vasseur, and P. Merriaux, "Millimeter wave FMCW RADARs for perception, recognition and localization in automotive applications: A survey," *IEEE Transactions on Intelligent Vehicles*, Vol. 7, No. 3, 533–555, 2022.
3. Zhang, Z., Z. Tian, and M. Zhou, "Latern: Dynamic continuous hand gesture recognition using FMCW radar sensor," *IEEE Sensors Journal*, Vol. 18, No. 8, 3278–3289, 2018.
4. Wang, G., J. -M. Muñoz-Ferreras, C. Gu, C. Li, and R. Gómez-García, "Application of linear-frequency-modulated continuous-wave (LFMCW) radars for tracking of vital signs," *IEEE Transactions on Microwave Theory and Techniques*, Vol. 62, No. 6, 1387–1399, 2014.
5. Zhou, Z., Y. Li, J. Hu, Y. He, Z. Zhang, and P.-Y. Chen, "Monostatic copolarized simultaneous transmit and receive (STAR) antenna by integrated single-layer design," *IEEE Antennas and Wireless Propagation Letters*, Vol. 18, No. 3, 472–476, 2019.
6. Wu, D., Y. -X. Sun, B. Wang, and R. Lian, "A compact, monostatic, co-circularly polarized simultaneous transmit and receive (STAR) antenna with high isolation," *IEEE Antennas and Wireless Propagation Letters*, Vol. 19, No. 7, 1127–1131, 2020.
7. Liu, Y., Z. Yue, Y. Jia, Y. Xu, and Q. Xue, "Dual-band dual-circularly polarized antenna array with printed ridge gap waveguide," *IEEE Transactions on Antennas and Propagation*, Vol. 69, No. 8, 5118–5123, 2021.
8. Lei, H., Y. Liu, Y. Jia, Z. Yue, and X. Wang, "A low-profile dual-band dual-circularly polarized folded transmitarray antenna with independent beam control," *IEEE Transactions on Antennas and Propagation*, Vol. 70, No. 5, 3852–3857, 2022.
9. Liang, Z.-X., D.-C. Yang, X.-C. Wei, and E.-P. Li, "Dual-band dual circularly polarized microstrip antenna with two eccentric rings and an arc-shaped conducting strip," *IEEE Antennas and Wireless Propagation Letters*, Vol. 15, 834–837, 2016.
10. Yan, Y.-D., Y.-C. Jiao, H.-T. Cheng, and C. Zhang, "A low-profile dual-circularly polarized wide-axial-ratio-beamwidth slot patch antenna with six-port feeding network," *IEEE Antennas and Wireless Propagation Letters*, Vol. 20, No. 12, 2486–2490, 2021.
11. Wu, J., W. Yang, L. Gu, Q. Xue, and W. Che, "Low-profile wide-band dual-circularly polarized metasurface antenna based on traveling-wave sequential feeding mechanism," *IEEE Antennas and Wireless Propagation Letters*, Vol. 21, 1085–1089, 2022.
12. Mao, C.-X., S. S. Gao, Y. Wang, and J. T. Sri Sumantyo, "Compact broadband dual-sense circularly polarized microstrip antenna/array with enhanced isolation," *IEEE Transactions on Antennas and Propagation*, Vol. 65, No. 12, 7073–7082, 2017.
13. He, Y., C. Gu, H. Ma, J. Zhu, and G. V. Eleftheriades, "Miniaturized circularly polarized doppler radar for human vital sign detection," *IEEE Transactions on Antennas and Propagation*, Vol. 67, No. 11, 7022–7030, 2019.
14. Lu, J., Z. Shao, C. Li, C. Gu, and J. Mao, "A portable 5.8GHz dual circularly polarized interferometric radar sensor for short-range motion sensing," *IEEE Transactions on Antennas and Propagation*, Vol. 70, No. 7, 5849–5859, 2022.
15. Li, H., L. Kang, F. Wei, Y.-M. Cai, and Y.-Z. Yin, "A low-profile dual-polarized microstrip antenna array for dual-mode OAM applications," *IEEE Antennas and Wireless Propagation Letters*, Vol. 16, 3022–3025, 2017.
16. Lu, J., Z. Kuai, X. Zhu, and N. Zhang, "A high-isolation dual-polarization microstrip patch antenna with quasi-cross-shaped coupling slot," *IEEE Transactions on Antennas and Propagation*, Vol. 59, No. 7, 2713–2717, 2011.

17. Chen, Z., L. Mei, L. Guo, Z. Wu, and M. Tang, "Isolation enhancement for wideband, circularly/dual-polarized, high-density patch arrays using planar parasitic resonators," *IEEE Access*, Vol. 7, 112249–112257, 2019.
18. Ta, S., V. Nguyen, B. Nguyen-Thi, T. Hoang, A. Nguyen, K. Nguyen, and C. Dao-Ngoc, "Wideband dual-circularly polarized antennas using aperture-coupled stacked patches and single-Section hybrid coupler." *IEEE Access*, Vol. 10, 21883–21891, 2022.